Supplementary Information

Understanding the spin effects of single-atom alloys on the electrocatalytic nitrogen reduction reaction

Yiming Ren[+], Peiyao Bai[+], Shilin Wei and Lang Xu*

MOE Key Laboratory of Coal Processing and Efficient Utilization, School of Chemical Engineering and Technology, China University of Mining and Technology, 1 Daxue Road, Xuzhou, Jiangsu, 221116, China

[*] Corresponding author. *E-mail address: lang.xu@cumt.edu.cn* (L. Xu).

[+] Both authors contributed equally to this work.

This file includes:

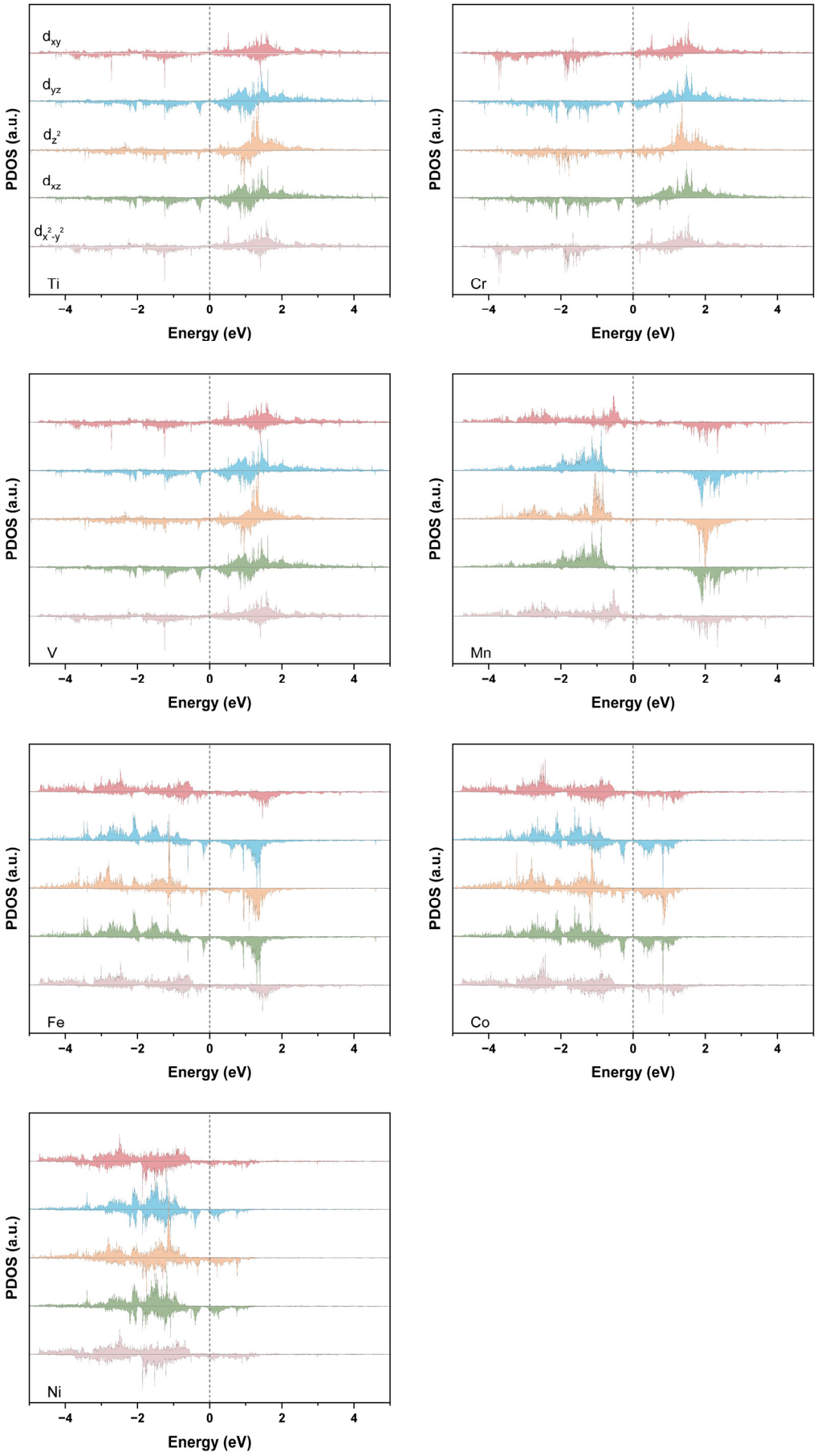

Fig. S1 | d-Orbital projected density of states of the dopants in the fourth-period Co-SAAs.

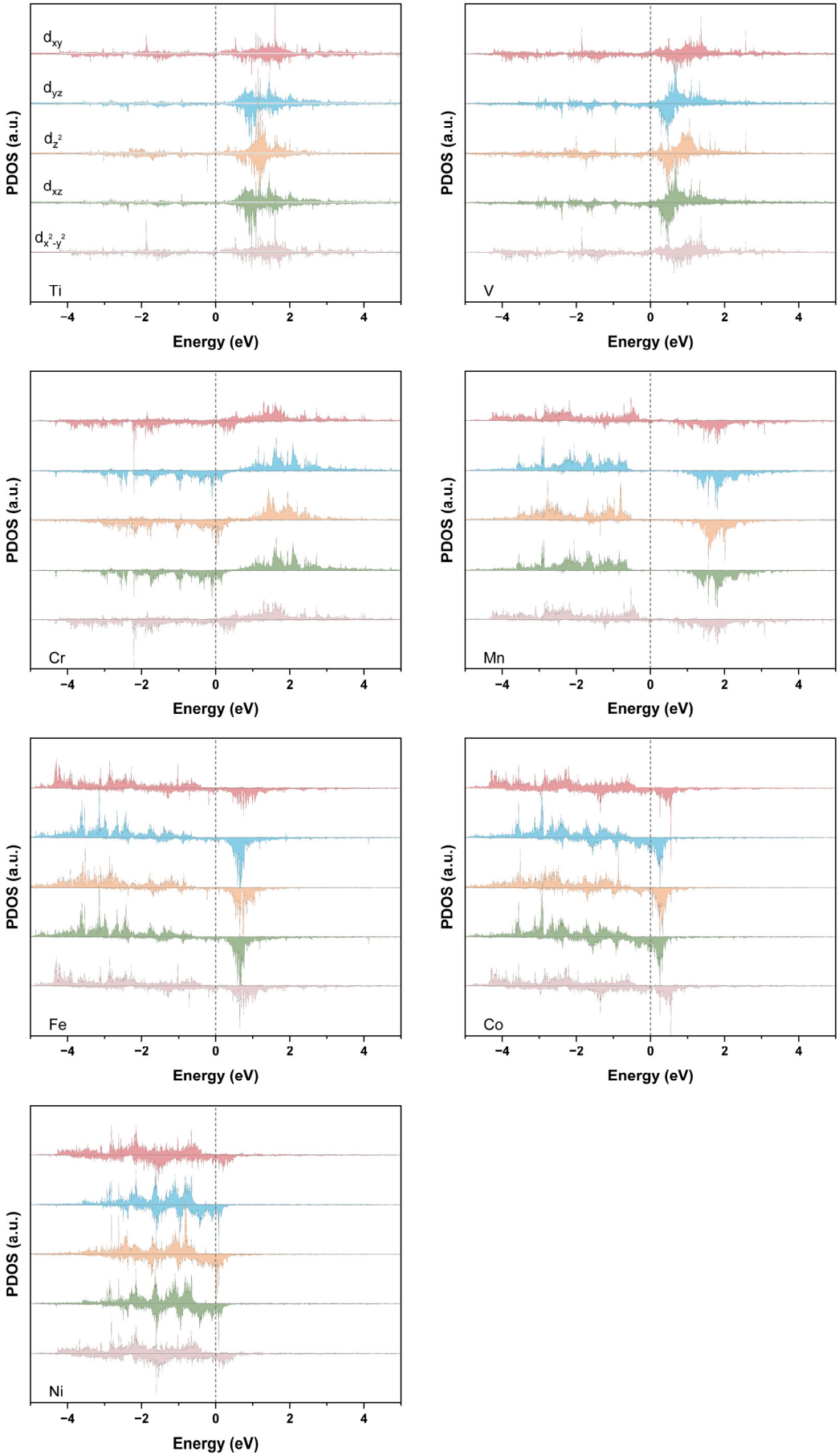

Fig. S2 | d-Orbital projected density of states of the dopants in the fourth-period Ni-SAAs.

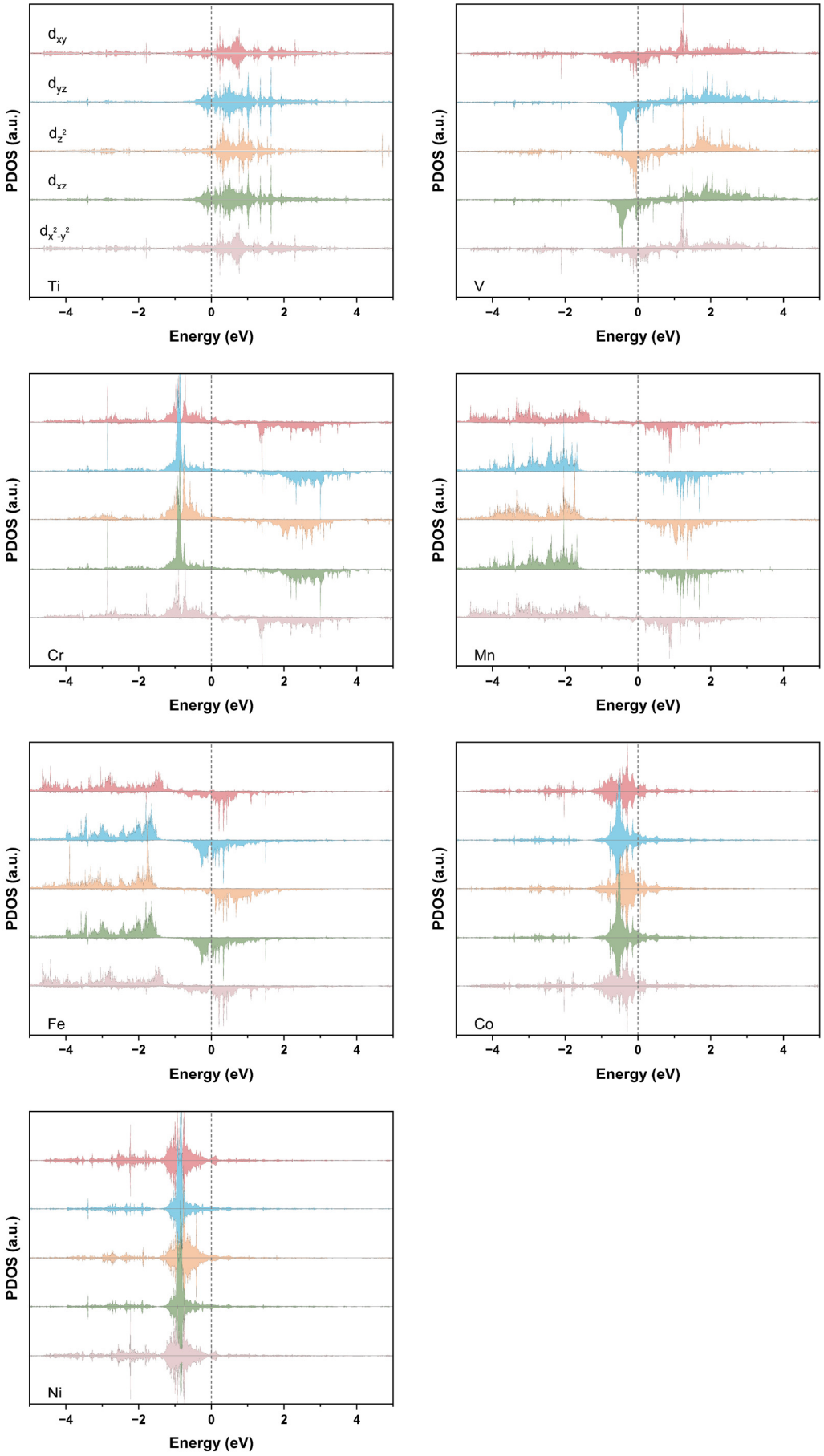

Fig. S3 | d-Orbital projected density of states of the dopants in the fourth-period Cu-SAAs.

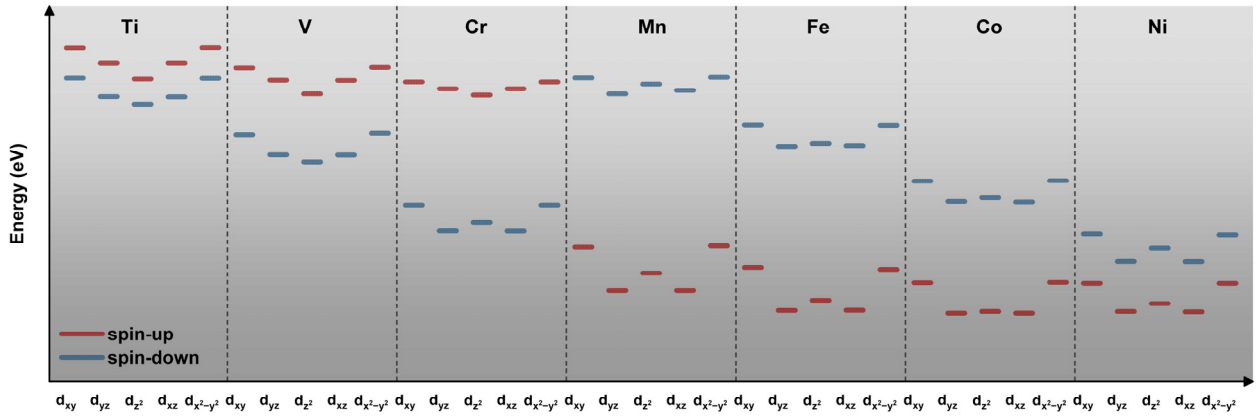

Fig. S4 | d-Orbital degeneracies and arrangements of the dopants in the fourth-period Co-SAAs; the d-orbital energy levels are approximated by ε_d^W.

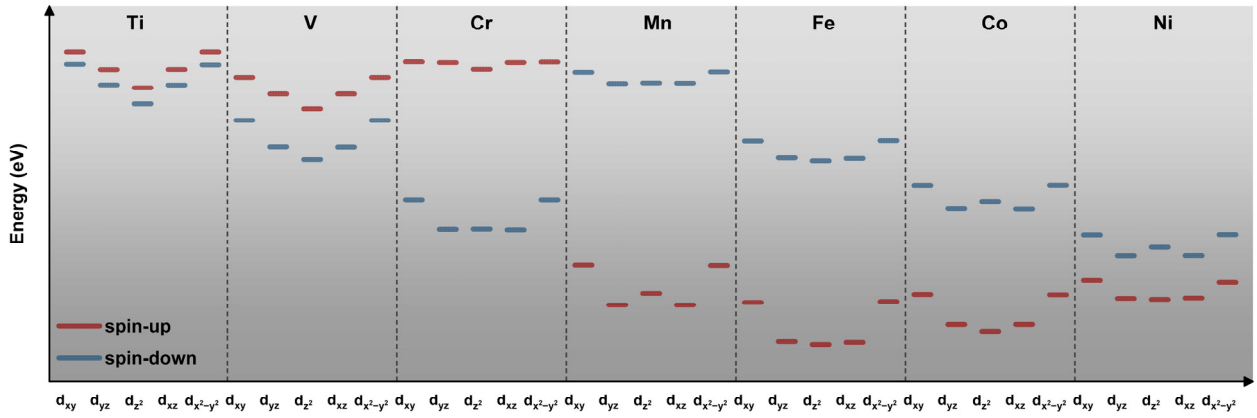

Fig. S5 | d-Orbital degeneracies and arrangements of the dopants in the fourth-period Ni-SAAs; the d-orbital energy levels are approximated by ε_d^W.

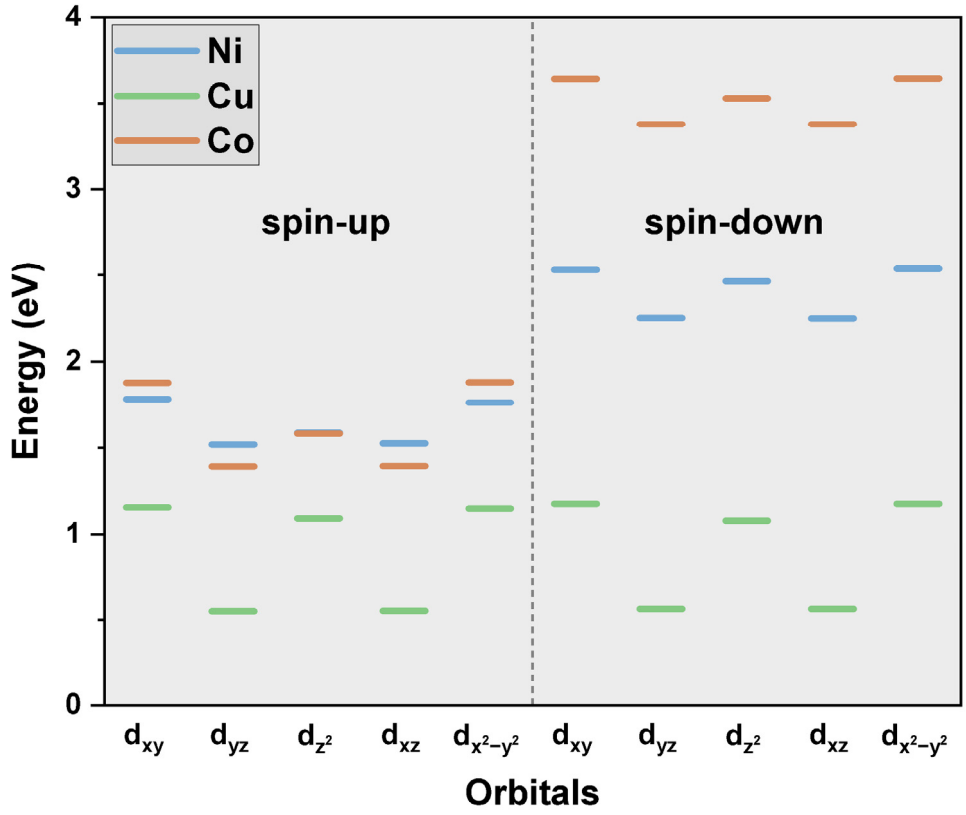

Fig. S6 | d-Orbital degeneracies and energy levels (ε_d^W) for an atom on Co(111), Ni(111) and Cu(111) metal surfaces.

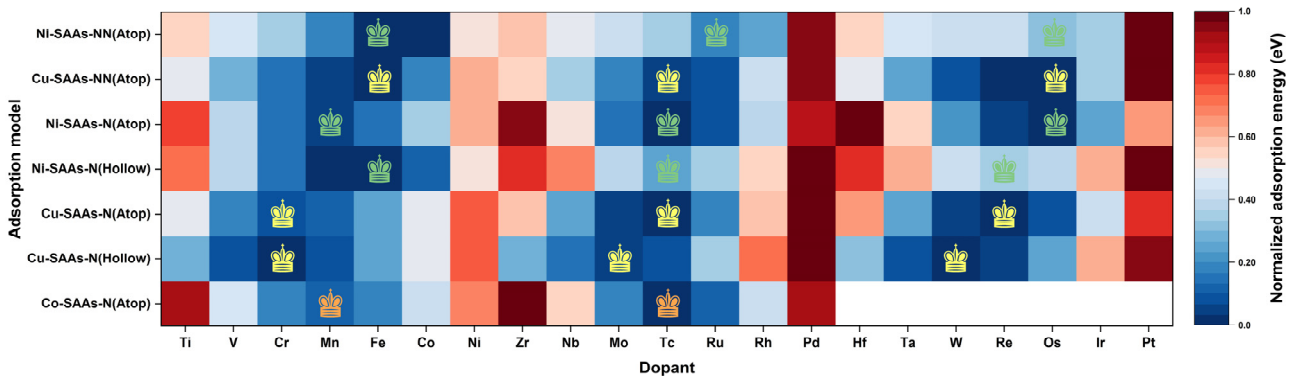

Fig. S7 | A heatmap of the adsorption energies of Co-SAAs, Ni-SAAs and Cu-SAAs for N atoms and N_2 molecules by NSP calculations, with adsorption energy values being normalized.

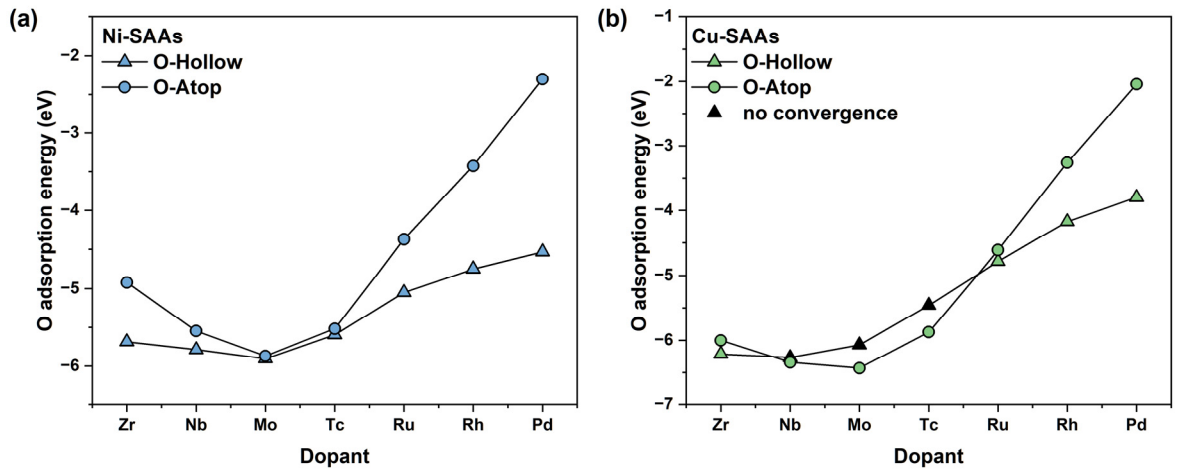

Fig. S8 | Oxygen-atom adsorption energies of the fifth-period (a) Ni-SAAs and (b) Cu-SAAs with Atop and Hollow adsorption configurations.

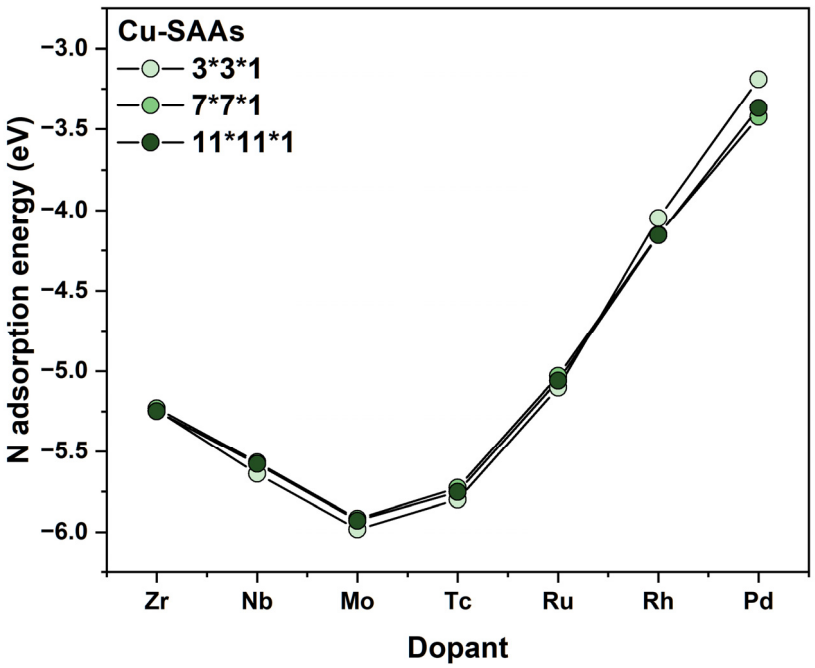

Fig. S9 | Adsorption energies of the fifth-period Cu-SAAs for N atom (with Hollow configuration) by DFT calculations with different densities of k-points.

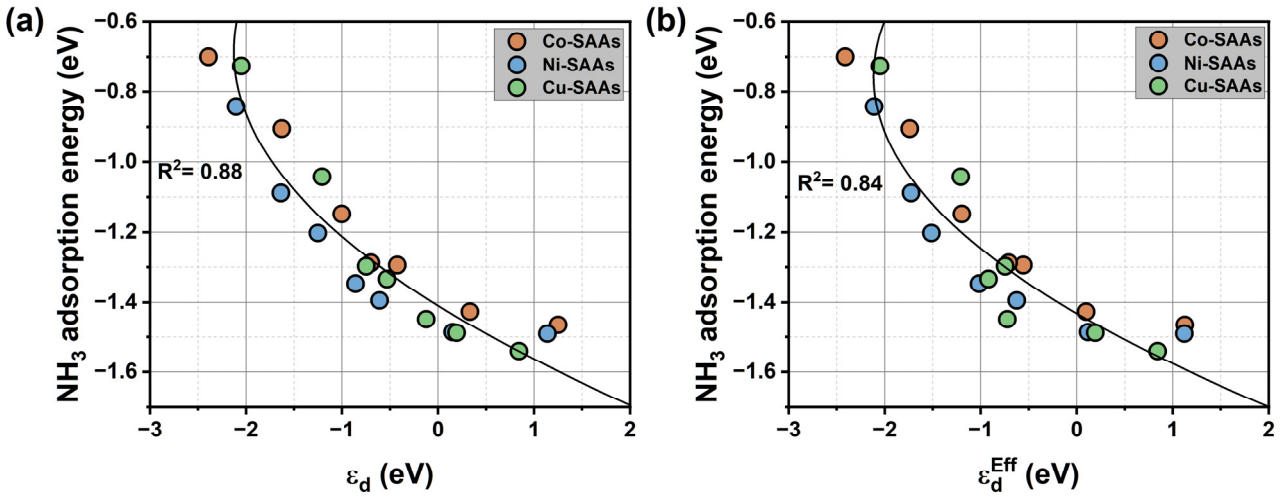

Fig. S10 | Relationships between NH_3 adsorption energies of SAAs and (a) d-band centers (ε_d) and (b) effective d-band centers (ε_d^{eff}) of the dopants.

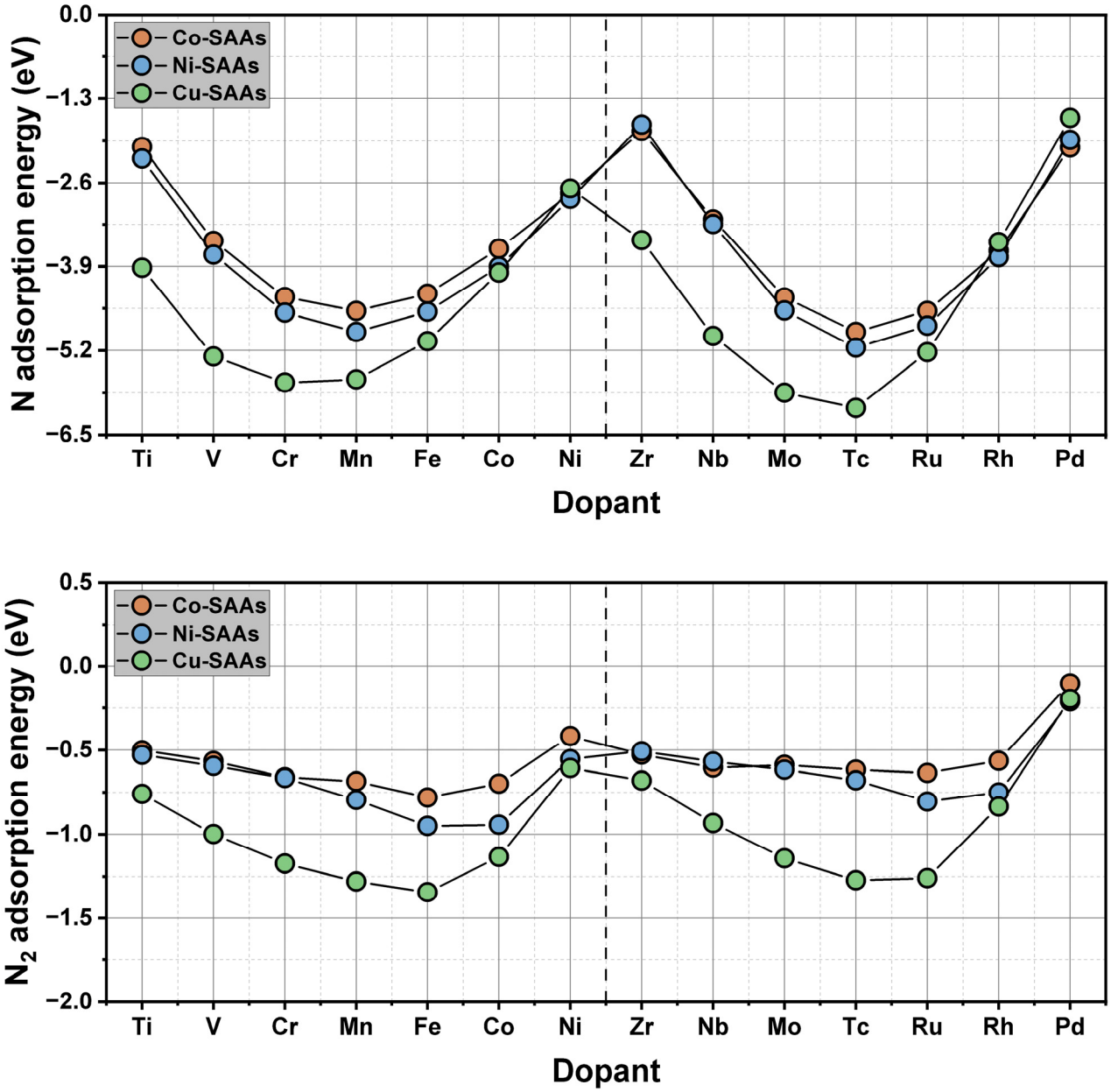

Fig. S11 | Adsorption energies of SAAs for N atom and N_2 molecule by NSP calculations.

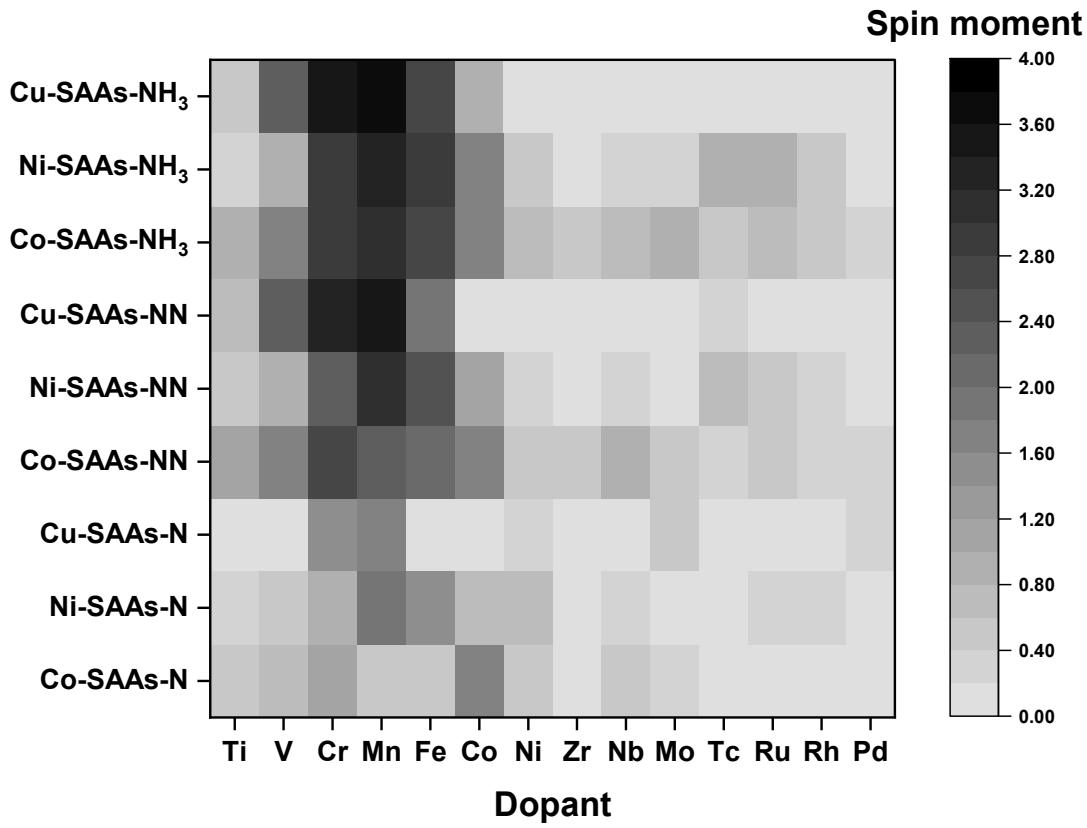

Fig. S12 | Absolute values of spin moments of the dopants in SAA–adsorbate systems.

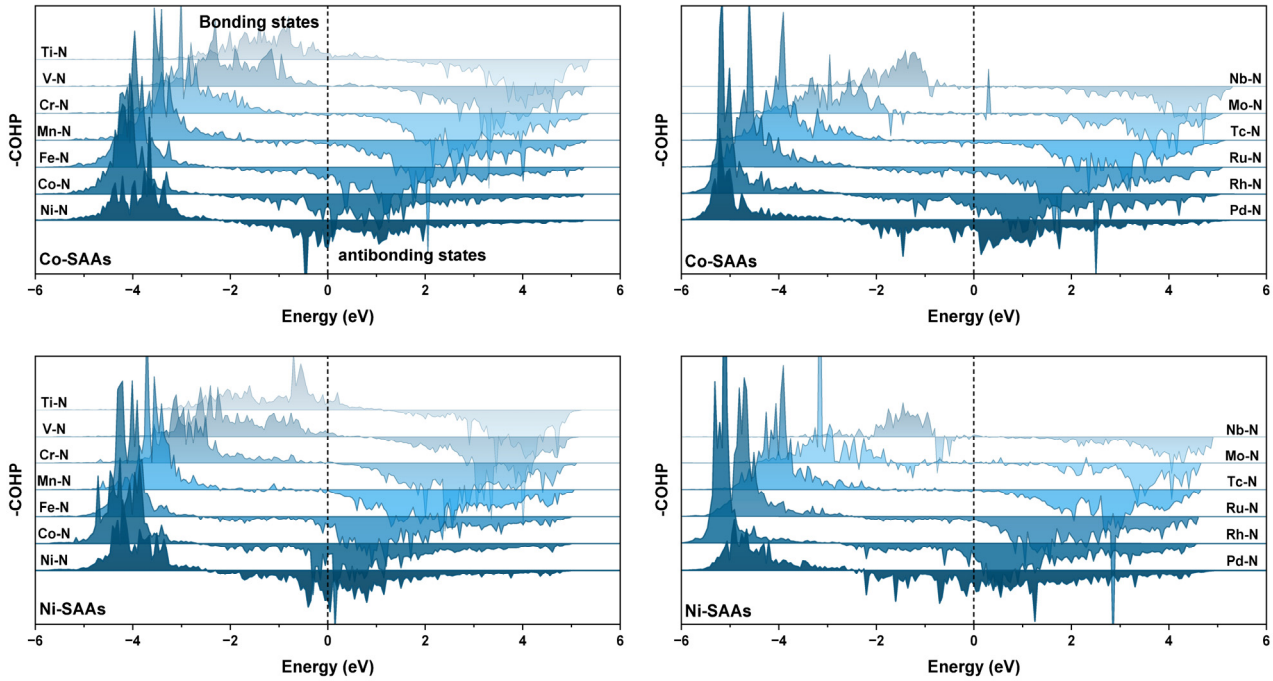

Fig. S13 | COHP diagrams of the dopant–N bonding for the fourth- and fifth-period Co-SAAs and Ni-SAAs.

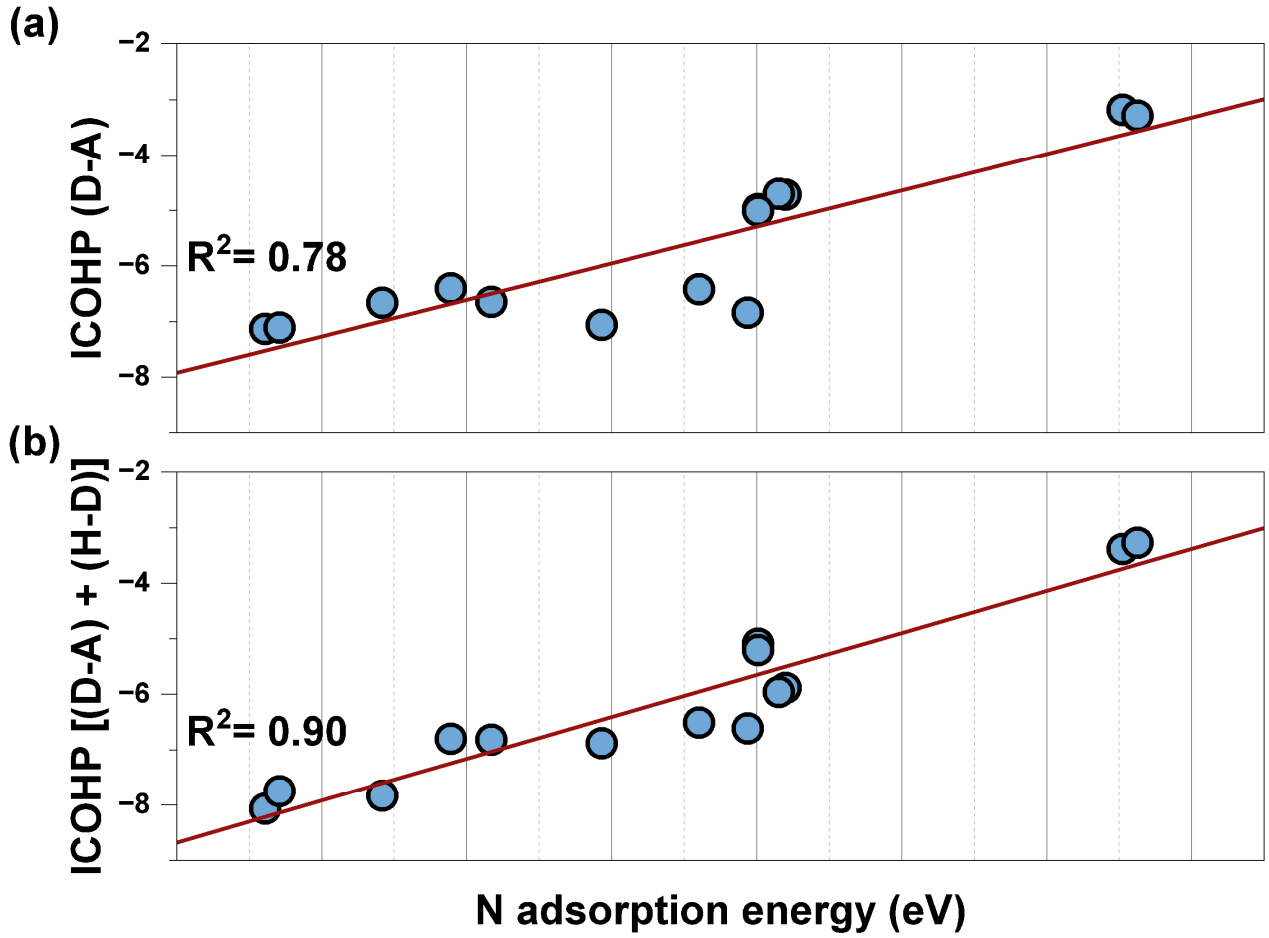

Fig. S14 | Scaling relationships (a) between ICOHP values of the D–A interaction and N adsorption energies, as well as (b) between the sum of ICOHP values of the D–A and D–H interactions and N adsorption energies for the fourth-period Cu-SAAs by SP and NSP calculations.

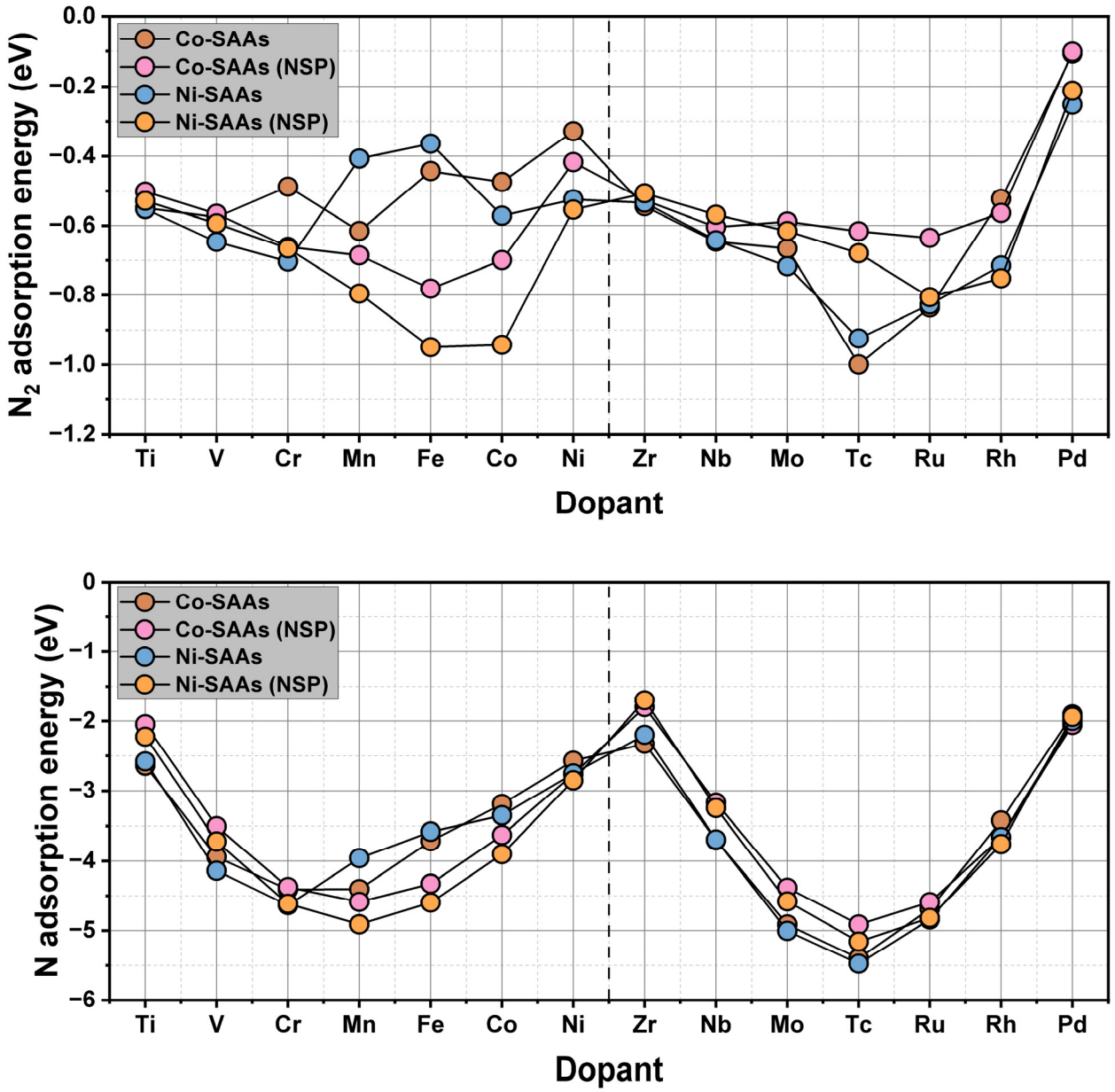

Fig. S15 | Adsorption energies of Co-SAAs and Ni-SAAs for N atom and N_2 molecule by SP and NSP calculations.

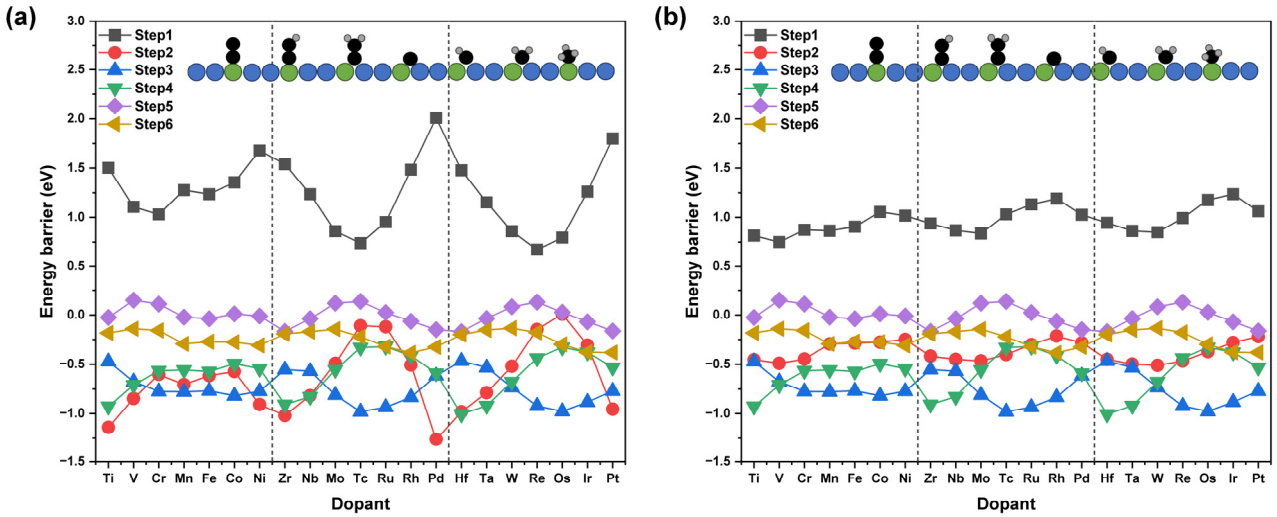

Fig. S16 | Energy barriers for the PCET steps during the e-NRR on Ni-SAAs. The NNH intermediate is adsorbed on the (a) Atop or (b) fcc site.

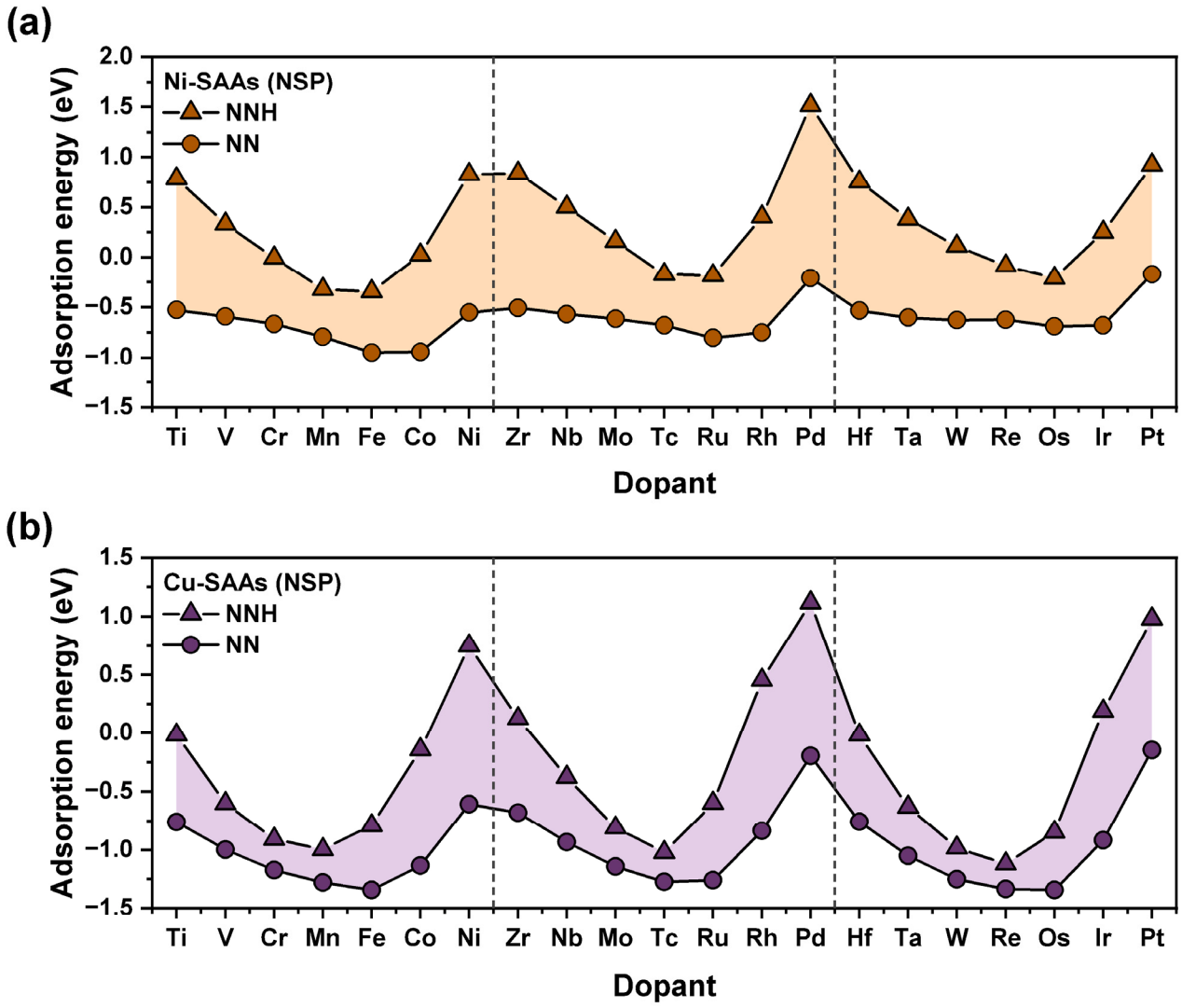

Fig. S17 | Adsorption energies of (a) Ni-SAAs and (b) Cu-SAAs for NN and NNH intermediates by NSP calculations.

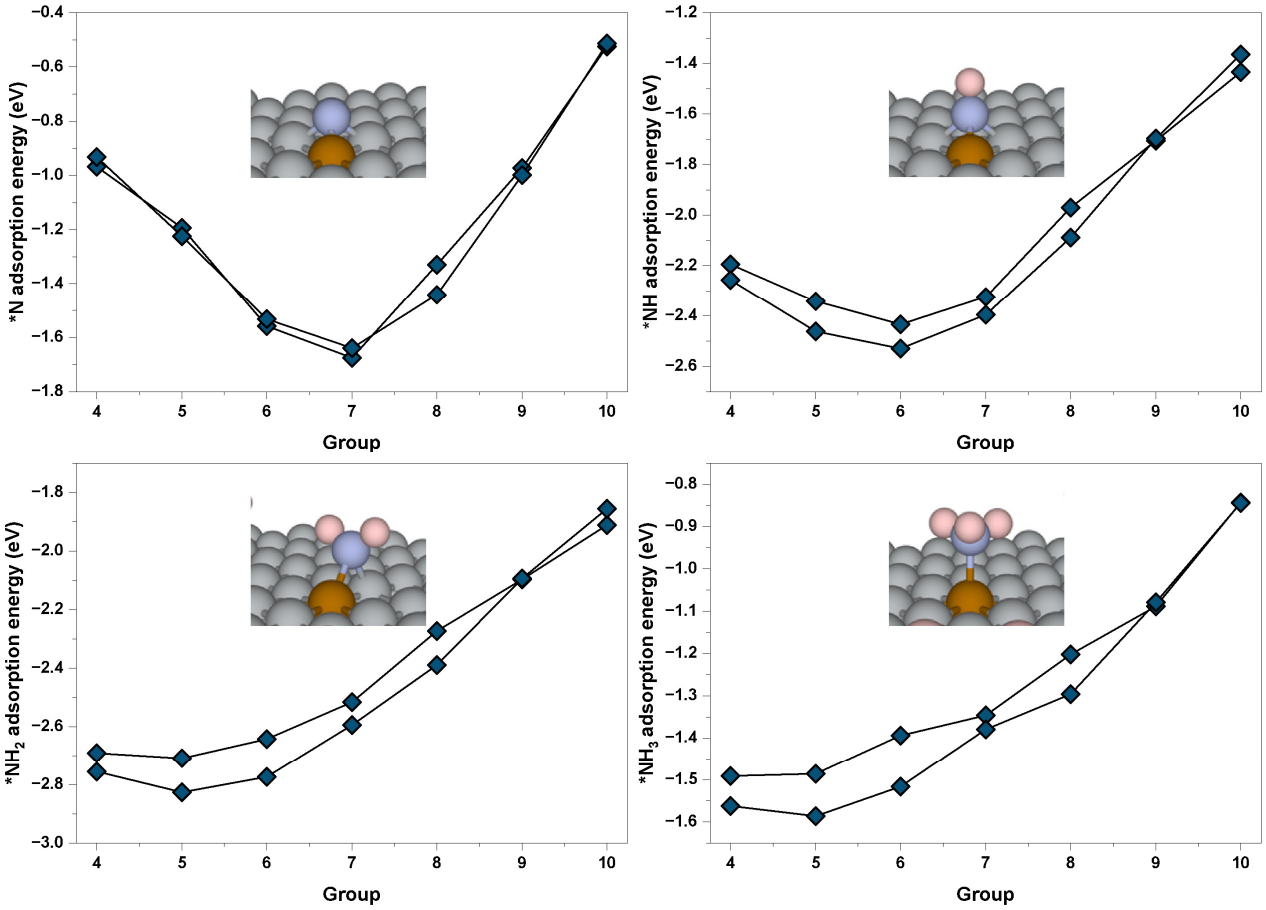

Fig. S18 | Adsorption energies of the fifth- and sixth-period Ni-SAAs for N, NH, NH_2 and NH_3 intermediates.

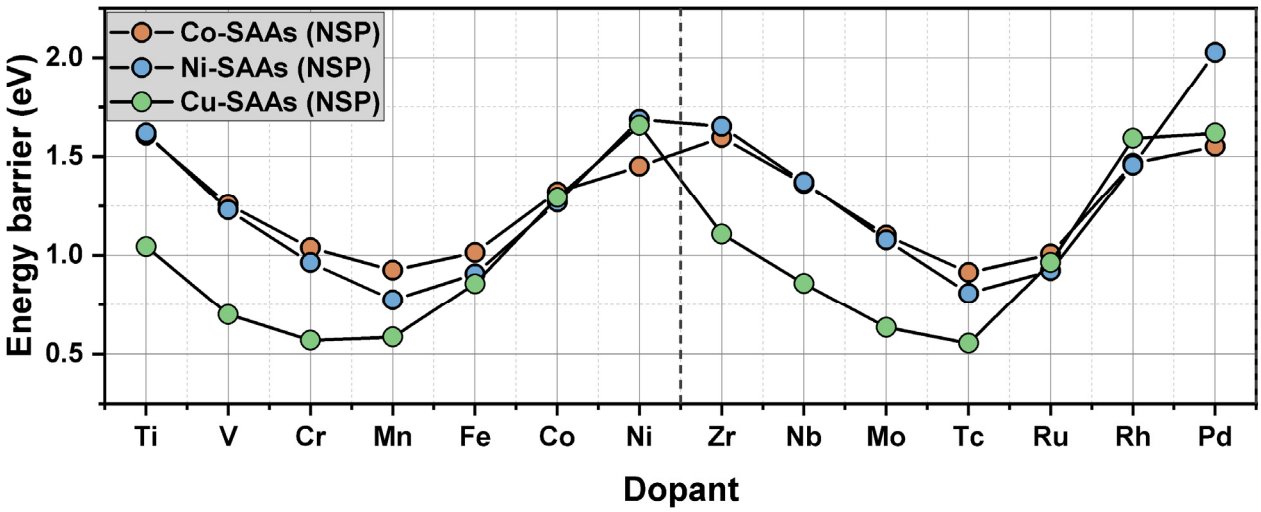

Fig. S19 | Energy barriers of PDS of the fourth- and fifth-period SAAs in the e-NRR process by NSP calculations.

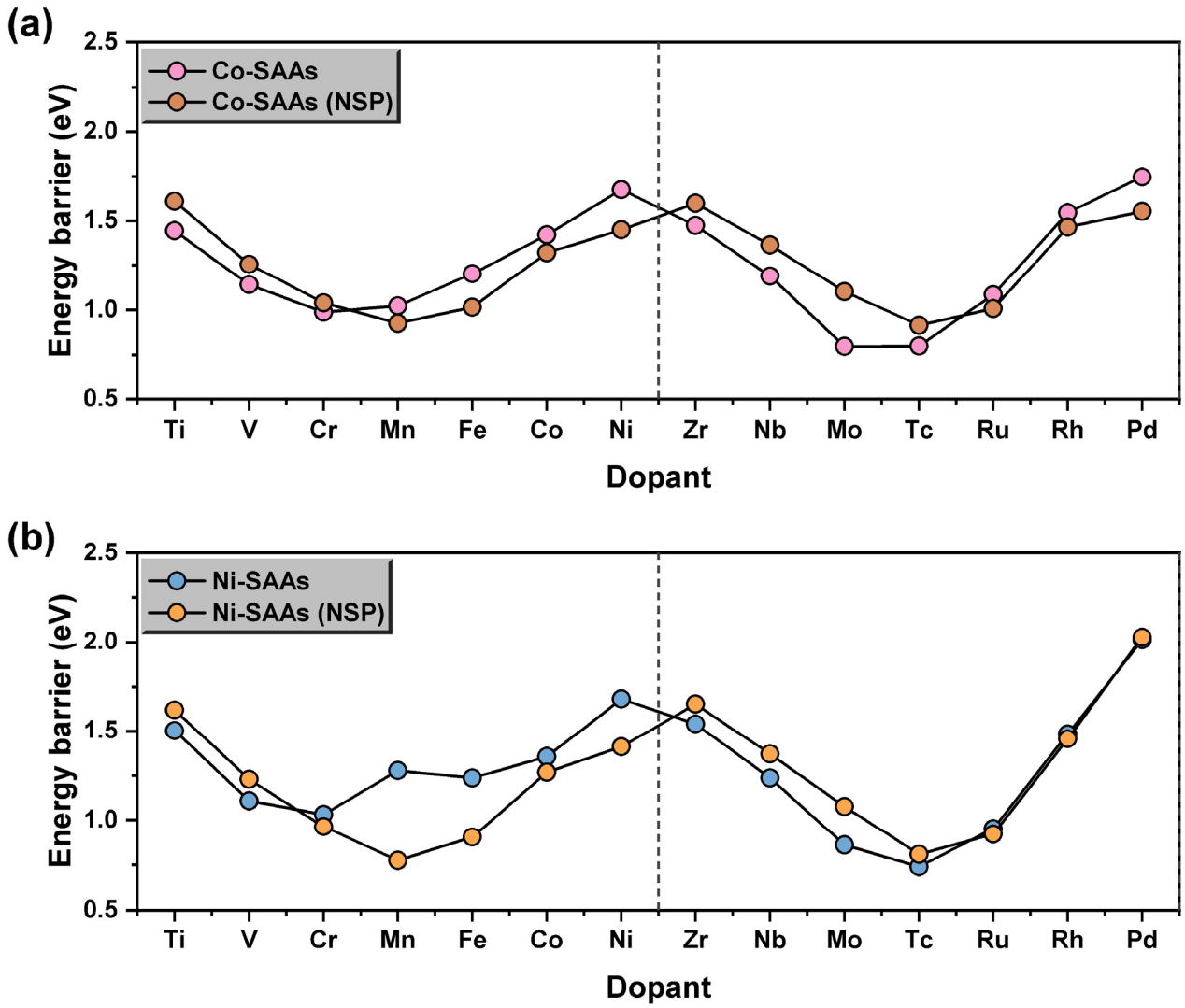

Fig. S20 | Energy barriers of PDS of the fourth- and fifth-period (a) Co-SAAs and (b) Ni-SAAs in the e-NRR by SP and NSP calculations.

Table S1 | DFT energies and corresponding free-energy correction values of atoms and molecules calculated at 298.15 K and 1 bar (or 0.035 bar for H_2O).

Adsorbate	***E*** **(eV)**	***H*** **(eV)**	***TS*** **(eV)**	G_{cor} **(eV)**	**Δ*G*** **(eV)**
H_2 (g)	–6.99	0.36	0.40	–0.04	–7.03
O	–1.96	0.06	0.47	–0.41	–2.36
N	–3.17	0.06	0.47	–0.41	–3.58
C	–1.39	0.06	0.46	–0.40	–1.79
N_2 (g)	–16.27	0.24	0.59	–0.35	–16.62
NH_3 (g)	–19.49	1.02	0.60	0.42	–19.07
CO (g)	–14.43	0.22	0.61	–0.39	–14.82
H_2O (l)	–14.15	0.67	0.58	0.00	–14.15

Table S2 | The GBR hyper-parameter settings when the target variables are the N adsorption energy of SAAs and the PDS energy barrier of SAAs in the e-NRR.

Hyper-parameters	N adsorption energy (eV)	PDS energy barrier (eV)
n_estimators	200	200
max_depth	2	2
learning_rate	0.15	0.15
min_samples_split	5	5
min_samples_leaf	5	3
max_leaf_nodes	4	3
max_features	0.7	0.7
subsample	0.8	0.8

Table S3 | The XGBR hyper-parameter settings when the target variables are the N adsorption energy of SAAs and the PDS energy barrier of SAAs in the e-NRR.

Hyper-parameters	N adsorption energy (eV)	PDS energy barrier (eV)
n_estimators	500	200
max_depth	5	3
learning_rate	0.15	0.2
min_child_weight	3	3
colsample_bytree	0.6	0.6
subsample	0.8	0.8

Table S4 | The interplanar spacing of SAA surface (D_h, Å) and the distance between dopants in periodic repeated surfaces (D_d, Å).

Dopant	Co-SAAs		Ni-SAAs		Cu-SAAs	
	D_h	D_d	D_h	D_d	D_h	D_d
Ti	2.16	9.81	2.11	9.79	2.16	10.05
V	2.14	9.81	2.12	9.79	2.16	10.04
Cr	2.15	9.81	2.11	9.79	2.15	10.04
Mn	2.14	9.80	2.11	9.79	2.17	10.05
Fe	2.14	9.81	2.12	9.79	2.17	10.03
Co	2.12	——	2.12	9.78	2.18	10.00
Ni	2.13	9.80	2.12	——	2.17	10.01
Zr	2.17	9.81	2.11	9.81	2.15	10.05
Nb	2.18	9.82	2.10	9.80	2.15	10.05
Mo	2.17	9.81	2.11	9.79	2.15	10.05
Tc	2.16	9.82	2.11	9.79	2.15	10.03
Ru	2.17	9.82	2.11	9.80	2.15	10.02
Rh	2.17	9.82	2.10	9.81	2.15	10.03
Pd	2.18	9.83	2.10	9.81	2.15	10.04
Hf	2.18	9.81	2.10	9.80	2.15	10.05
Ta	2.18	9.82	2.11	9.80	2.16	10.06
W	2.16	9.81	2.11	9.79	2.16	10.04
Re	2.15	9.82	2.12	9.80	2.17	10.04
Os	2.16	9.82	2.11	9.80	2.16	10.02
Ir	2.17	9.82	2.11	9.80	2.16	10.02
Pt	2.18	9.83	2.10	9.81	2.15	10.04

Table S5 | Relevant features of dopants in SAAs.

Feature	Symbol
Atomic number	Z_d
Binding energy	E_b
Spin-up d-band center	ε_d^{up}
Spin-up d-band width	W_d^{up}
Spin-down d-band center	ε_d^{down}
Spin-down d-band width	W_d^{down}
d-electron	N_e
Effective d-band center	ε_d^{eff}
Spin moment of dopant after N adsorption	μ_B
Change in spin moment of dopant before and after N adsorption	$\Delta\mu_B$
N adsorption energy	$N.A.E$
N_2 adsorption energy	$NN.A.E$

References

1. C. D. Taylor, S. A. Wasileski, J. S. Filhol and M. Neurock, *Phys. Rev. B*, 2006, **73**, 165402.

2. K. Mathew, R. Sundararaman, K. Letchworth-Weaver, T. A. Arias and R. G. Hennig, *J. Chem. Phys.*, 2014, **140**, 084106.

3. K. Mathew, V. S. C. Kolluru, S. Mula, S. N. Steinmann and R. G. Hennig, *J. Chem. Phys.*, 2019, **151**, 234101.

4. G. Kresse and J. Furthmüller, *Phys. Rev. B*, 1996, **54**, 11169-11186.